Full paper/Mémoire

2-(7-methyl-1H-benzoimidazol-2-yl)-6-(1-aryliminoethyl) pyridinylnickel complexes: Synthesis, characterization and their ethylene oligomerization

Xia Chen [a,*], Liping Zhang [a,b], Tongling Liang [b], Xiang Hao [b], Wen-Hua Sun [b,*]

[a] School of Chemistry and Chemical Engineering, Shanxi University, Taiyuan 030006, China
[b] Key Laboratory of Engineering Plastics and Beijing National Laboratory for Molecular Science, Institute of Chemistry, Chinese Academy of Sciences, Beijing 100190, China

A R T I C L E   I N F O

A B S T R A C T

A series of 2-(methyl-substituted-1H-benzoimidazol-2-yl)-6-(1-aryliminoethyl)pyridines (**L1–L6**) were synthesized and used as $N^\wedge N^\wedge N$ tridentate ligands for their nickel complexes (**C1–C12**). All ligands were fully characterized by elemental, NMR and IR spectroscopic analyses, while their nickel complexes were characterized by elemental and IR spectroscopic analyses. The single-crystal X-ray diffraction reveals that the complexes **C1**, **C3** and **C9** have distorted octahedral geometry around the Ni center. All nickel complexes, activated with Et$_2$AlCl, exhibit good catalytic activities toward ethylene oligomerization with major dimerization.

© 2010 Académie des sciences. Published by Elsevier Masson SAS. All rights reserved.

1. Introduction

α-olefins are important substances used extensively for the detergents, synthetic lubricants, plasticizers, alcohols and comonomers used for branched polyolefins. The linear α-olefins were first manufactured by the Ziegler (Alfen) process in the presence of triethylaluminum (TEA). The large scale process developed as the SHOP process using nickel complex catalyst in the end of 1970s [1], and was successfully industrialized in the 1980s [2–4]. From the middle of 1990s, the late-transition metal complex catalysts have attracted great attention in olefin reactivity [5]; therefore the nickel complexes in ethylene oligomerization [6,7] have been resurrected. As far as efficient catalytic systems are expected, nickel complexes bearing bidentate ligands such as $N^\wedge N$ [8–10], $N^\wedge O$ [11,12] and $P^\wedge N$ [13,14] have been extensively studied. Within ferrous and cobaltous complexes acting as catalysts [15–20], various

tridentate $N^\wedge N^\wedge N$ ligands have been prepared. Interestingly, some $N^\wedge N^\wedge N$ tridentate nickel complexes show nice activities for either ethylene oligomerization or polymerization [21–25]. Various tridentate nickel complexes have been focused in our group, and most of them showed good to high catalytic activity towards ethylene reactivity [26–30].

In order to improve catalytic activities of metal complexes and finely tune their products, the useful way is to modify ligands through different substituents on the frame of ligands. Regarding catalysts employing iminopyridines, it is common to prepare derivatives of ligands through the condensation reaction using anilines bearing different substituents. It is a challenge and more promising to have the frame of ligands substituted. Recently, we explored metal complexes ligated by 2-(benzimidazole)-6-(1-arylimino-ethyl)pyridines (Scheme 1), all of their metal (iron, cobalt or nickel) complexes showed high activities up to 10^7 g.mol^{-1} (M)·h^{-1} for ethylene oligomerization [20,31–36]. Considering the influence of substituents linked on to N-atom of benzimidazole, the nickel complexes containing N–H in the benzimidazole ring [34] showed better catalytic activities than their analogues containing alkyl-substituents

---

* Corresponding author.
  E-mail addresses: chenxia@sxu.edu.cn (X. Chen), whsun@iccas.ac.cn (W.-H. Sun).
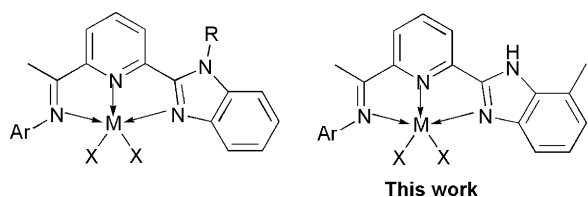
Scheme 1. Variation of Catalyst Models.

[32,33]. Such phenomena also appeared in their analogue iron complexes [20,31,33] and chromium complexes [35,36].

It is very difficult to further modify the imidazole ring of benzimidazole; therefore the functionalization of benzimidazole will be fused with the benzene ring. Keeping this idea in mind, the 6-(7-methyl-1H-benzoimidazol-2-yl)-2-acetylpyridine and its isomer 6-(4-methyl-1H-benzoimidazol-2-yl)-2-acetylpyridine were newly synthesized according to our developed procedure [31]. A series of 2-(benzimidazol-2-yl)-6-(1-aryliminoethyl)pyridines was

prepared and used to synthesize the nickel complexes of the title (Scheme 1). The nickel complexes showed good catalytic activities toward ethylene oligomerization using Et₂AlCl as cocatalyst. The effects of substituents on the ligands, the Al/Ni molar ratio, and reaction temperature on their catalytic activities and resultant oligomers have been investigated in detail. Herein the syntheses and characterizations these title nickel complexes are reported, along with the study of their catalytic activities towards ethylene oligomerization.

2. Results and discussion

2.1. Synthesis and characterization of ligands and complexes

The starting compound 6-(methyl-substituted-1H-benzo-imidazol-2-yl)-2-acetylpyridine was synthesized according to our previous procedure (Scheme 2) [31]. There are two isomers of the product obtained, the 6-(7-methyl-1H-benzoimidazol-2-yl)-2-acetylpyridine and 6-(4-methyl-1H-benzoimidazol-2-yl)-2-acetylpyridine
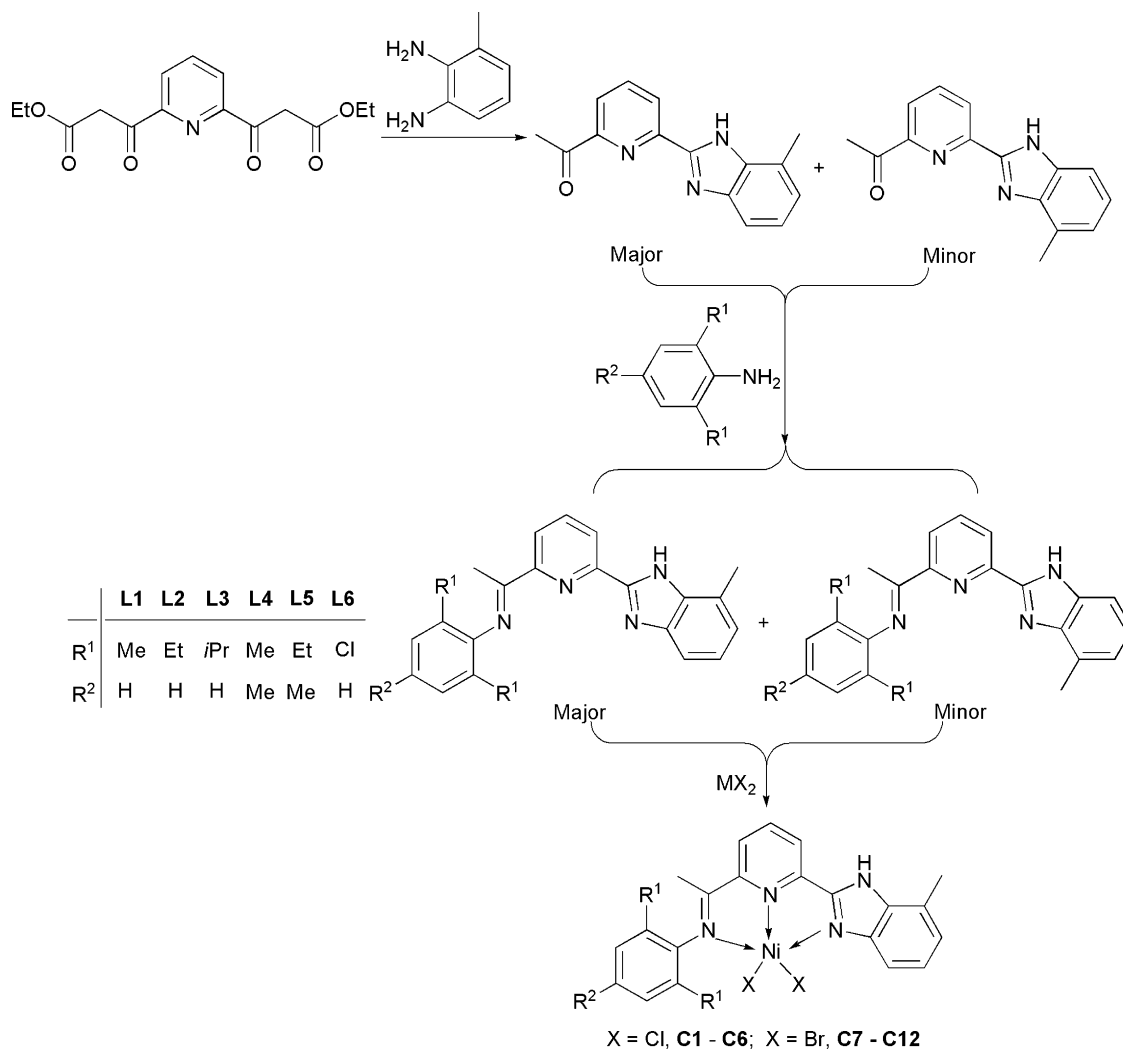
Scheme 2. Synthesis of nickel complexes.

approximately in the ratio of 3:2 based on the ^{1}H NMR spectrum. However, they were not separated by column chromatography. The ligands **L1**–**L6** were prepared by treating the starting substance with corresponding aniline in toluene (Scheme 2) according to our previous procedure [37]. All of them were similarly isomerized in two configurations in the ratios about of 3:2. On the base of the ^{1}H NMR measurement in the CDCl$_3$ solution, ligand **L5** within the range of 25 °C to 55 °C, there is no significant difference to indicate different ratios of isomes. All these compounds are stable in solid state, and fully characterized by elemental analysis, FT-IR, ^{1}H and ^{13}C NMR.

The dichloronickel(II) complexes (**C1**–**C6**) were prepared by the stoichiometric reactions of the appropriate ligands with NiCl$_2$·6H$_2$O in ethanol for 12 h. The equimolar interactions of **L1**–**L6** with (DME)·NiBr$_2$ in tetrahydrofuran (THF) for 12 h gave dibromonickel(II) complexes (**C7**–**C12**) (Scheme 2). All the nickel(II) complexes of the title obtained are air-stable, yellow in color and in good yields (65–95%). Their IR spectra showed absorption bands between 1590 and 1560 cm^{-1}, which correspond to the ν (C = N) stretching frequencies about 50 cm^{-1} shifted to lower wavenumber in comparison with their free ligands. The single crystals of nickel complexes **C1**, **C3** and **C9** suitable for X-ray diffraction analysis were obtained by laying diethyl ether on their methanol solutions. Their complexes' analogues reported [30–36], the dibromonickel complexes coordinate with ligands in the N^N^N tridentate manner, in which the sp^2–hybridized nitrogen of benzoimidazole coordinated with nickel atom. The other isomer could not be figured out; both complexes were surprisingly observed as one isomer with methyl-substituent far away to nickel center by the X-ray diffraction analysis (Scheme 2). The favorable structures of nickel complexes were formed due to the steric hindrance of the methyl-substituent on the benzoimidazole along with its proton immigrated within the benzoimidazole.

The coordination geometry of complexes **C1** and **C3** could be described as distorted octahedral including one coordinated methanol, individually. In addition, there are independent methanol molecules in the crystal cell of the complex **C1**. The molecular structure of **C1·CH$_3$OH** is shown in Fig. 1, and the selected bond lengths and angles are tabulated in Table 1. In the molecular structure of
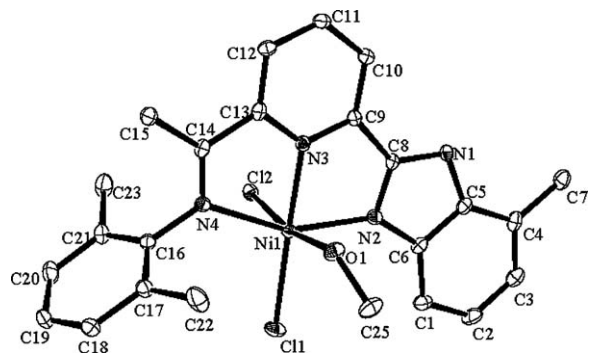

Fig. 1. ORTEP Molecular structure of **C1·CH$_3$OH**. Thermal ellipsoids are shown at 30% probability level. Hydrogen atoms have been omitted for clarity.

Table 1
Selected bond lengths and Angles for **C1·CH$_3$OH** and **C3·CH$_3$OH**.

	C1·CH$_3$OH	**C3·CH$_3$OH**
	Bond lengths (Å)	
Ni–N$_2$	2.097(5)	2.117(3)
Ni–N$_3$	2.013(5)	2.023(3)
Ni–N$_4$	2.197(5)	2.214(3)
Ni–Cl$_1$	2.2924(17)	2.3187(10)
Ni–Cl$_2$	2.5237(18)	2.4112(11)
N$_1$–C$_8$	1.356(7)	1.357(4)
N$_2$–C$_8$	1.324(7)	1.332(4)
N$_4$–C$_{14}$	1.287(8)	1.284(4)
Ni–O	2.160(4)	2.174(3)
	Bond angles (°)	
N$_2$–Ni–N3	78.74(19)	78.30(11)
N$_2$–Ni–N4	155.23(18)	153.78(11)
N$_3$–Ni–N4	76.50(18)	75.98(11)
N$_2$–Ni–Cl$_1$	101.02(14)	102.88(8)
N$_3$–Ni–Cl$_1$	176.65(15)	170.83(9)
N$_4$–Ni–Cl$_1$	103.66(13)	101.72(8)
Cl$_1$–Ni–Cl$_2$	96.45(7)	96.51(4)
N$_2$–Ni–Cl$_2$	89.15(14)	88.90(9)
N$_3$–Ni–Cl$_2$	86.89(14)	92.60(9)
N$_4$–Ni–Cl$_2$	90.26(13)	97.19(8)
O$_1$–Ni–Cl$_1$	92.23(13)	81.82(8)
O$_1$–Ni–Cl$_2$	169.86(12)	176.08(7)

C1·CH$_3$OH, the nickel atom deviates by 0.0182 Å from the plane formed by N(2), N(3) and N(4). The chlorine atom Cl(1) is almost in coplanar manner with deviation of 0.0947 Å, and the other chlorine atom Cl(2) deviates by 2.5367 Å from this plane in the opposite direction. The dihedral angle between the iminoaryl ring and the benzimidazole ring is 105.7°, the basal plane which formed by N(2), N(3), N(4) is nearly coplanar to the pyridine ring with the dihedral angle of 2.9°, and the dihedral angle between iminoaryl ring and the pyridine ring is 102.8°. The N(2)–C(8) (1.324(7) Å) is shorter than the N(1)–C(8) (1.356(7) Å), suggesting typical SP^2–N character of the coordinated nitrogen of the benzoimidazole. The three Ni–N bond lengths are Ni(1)–N(2) 2.097(5) Å, Ni(1)–N(3) 2.013(5) Å and Ni(1)–N(4) 2.197(5) Å, respectively. Beyond the coordinated methanol with Ni(1)–O(1) (2.160(4) Å), there are slight differences of Ni(1)–Cl(1) (2.2924(17) Å) and Ni(1)–Cl(2) (2.5237(18) Å). The differences of the O–Ni–Cl angles are 92.23(13)° and 169.86(12)°.

Like complex **C1**, the molecular structure of **C3·CH$_3$OH** (Fig. 2) also shows the six-coordinated geometry with coordination of solvent methanol molecule and two Cl atoms. The selected bond lengths and angles are tabulated in Table 1. The central nickel atom deviates by 0.1235 Å from the plane containing N(2), N(3), N(4), while the Cl(1) deviates by 0.0993 Å and Cl(2) deviates by 2.5276 Å in the opposite direction. The plane composed by N(2), N(3) and N(4) is almost coplanar to the pyridyl ring with dihedral angle of 2.3°, the pyridyl ring and the benzimidazole ring are also nearly coplanar with dihedral angle of 2.8°. The dihedral angles between the phenyl plane and the benzimidazole ring, and the phenyl plane with the pyridine ring are 95.5° and 96.9°, respectively. Due to the isopropyl group in complex **C3·CH$_3$OH** instead of methyl in complex **C1·CH$_3$OH** (Table 1), there are slightly longer Ni–N bond lengths observed for complex **C3** such as
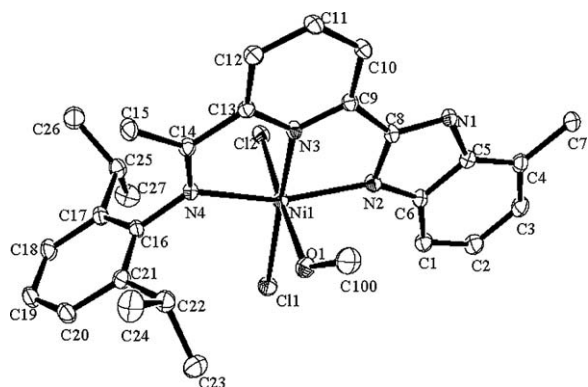
Fig. 2. ORTEP Molecular structure of **C3·CH₃OH**. Thermal ellipsoids are shown at 30% probability level. Hydrogen atoms have been omitted for clarity.

Ni(1)–N(2) 2.117(3) Å, Ni(1)–N(3) 2.023(3) Å and Ni(1)–N(4) 2.214(3) Å. The Ni–Cl bond lengths are closer: Ni(1)–Cl(1) (2.3187(10) Å) and Ni(1)–Cl(2) (2.4112(11) Å).

As shown in the Fig. 3, with the coordination of two methanol molecules, the coordination geometry of **[L3NiBr₂CH₃OH]Br** can be described as a distorted octahedron. In the single crystals of **[L3NiBr₂CH₃OH]Br**, one bromine atom of **C9** was replaced by one methanol molecule and acted as a counterion which was relatively far from the nickel center. The axial plane (O(1)–Ni(1)–O(2)) is nearly perpendicular to the equatorial plane which formed by N(2), N(3) and N(4) with a dihedral angle of 91.8°. The benzimidazole ring is nearly coplanar with the pyridine ring with a dihedral angle of 2.4°. Two O-atoms (O(1) and O(2)) of coordinated methanols located in mutually *trans*-positions form an angle of 176.39(13)° with the nickel core and the bond lengths of the O–Ni(1) are slightly different as O(1)–Ni(1) 12.068(3) Å and O(2)–Ni(1) 2.086(3) Å. The coordination geometry was observed in its
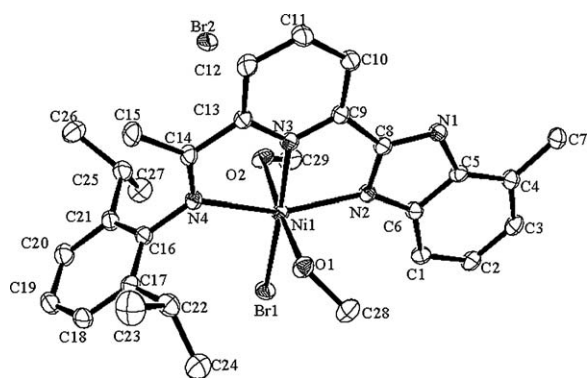

Fig. 3. ORTEP Molecular structure of **[L3NiBr₂CH₃OH]Br**. Thermal ellipsoids are shown at 30% probability level. Hydrogen atoms have been omitted for clarity. Selected bond lengths (Å) and angles (deg): Ni(1)–N(2) = 2.140(3), Ni(1)–N(3) = 2.016(3), Ni(1)–N(4) = 2.204(3), Ni(1)–Br(1) = 2.4742(9), Ni(1)–O(1) = 2.068(3), Ni(1)–O(2) = 2.086(3), N(2)–C(8) = 1.327(5), N(1)–C(8) = 1.348(5); N(3)–Ni(1)–N(2) = 78.46(13), N(3)–Ni(1)–N(4) = 76.14(13), N(2)–Ni(1)–N(4) = 154.57(12), O(1)–Ni(1)–O(2) = 176.39(13), N(3)–Ni(1)–O(1) = 90.82(14), N(3)–Ni(1)–O(2) = 86.99(13), O(1)–Ni(1)–N(2) = 88.73(13), O(2)–Ni(1)–N(2) = 88.03(13), O(1)–Ni(1)–N(4) = 90.38(12), O(2)–Ni(1)–N(4) = 91.87(12).

chloroanalogue ligated by 2-(1H-2-benzimidazolyl)-6-(1-(arylimino)ethyl)pyridines [34]. Compared with the chloroanalogue of **[L1NiCl(CH₃OH)₂]Cl** [34], the N–Ni bond lengths of **[L3NiBr₂CH₃OH]Br**, Ni(1)–N(2) = 2.140(3) Å, Ni(1)–N(3) = 2.016(3) Å and Ni(1)–N(4) = 2.204(3) Å, are within the typical values of coordination bonds [27,32,34].

In general, all the three complexes show the six-coordinated geometry around nickel atom with coordination of additional methanol molecules. The catalytic behaviors of all complexes are investigated with the prior dried precatalysts in order to avoid any solvent incorporated. The elemental analyses of their complexes are past after being dried under vacuum more than 4 h.

2.2. Ethylene oligomerization

The nickel (II) complexes **C1**–**C12** are systematically investigated for the oligomerization of ethylene with the Et₂AlCl as a cocatalyst. Because of low catalytic activity at ambient pressure of ethylene, the screening for catalysis is carried out at 10 atm of ethylene. Complex **C4** is typically investigated under a range of reaction conditions, such as molar ratios of cocatalyst to nickel and various temperature. The oligomers are only obtained and measured by GC. When the Al/Ni molar ratios of Et₂AlCl to **C4** are changed from 400 to 800 (Entries 1–4, Table 2), the catalytic activities first increase and then decrease. The optimum activity is observed at the Al/Ni molar ratio of 700. The influence of reaction temperatures on their catalytic activities are checked by the catalytic systems of **C4** (Entries 3 and 5–7, Table 2) and **C10** (Entries 21–24, Table 2). The highest activity is obtained at 30 °C (Entries 3 and 22, Table 2), and higher temperatures led to an obvious decrease of the catalytic activity. At room temperature, it is observed a little lower catalytic activity (Entries 5 and 21, Table 2) than that at 30 °C. It is assumed that the lower temperature do not activate active sites or relative lower movements of reactive substances. Meanwhile, decomposition of some active centers or unfavorable intermediates formed might happen along with a lower solubility of ethylene in toluene at higher temperature. Such phenomena have also observed in their analogue complexes [31–36]. Regarding lifetime of active species, the catalytic reactions are terminated within different reaction periods of the catalytic system of complex **C4** (Entries 8–12, Table 2). The higher activities are observed in shorter reaction times; the highest in 10 mins, on the other hand, activities are decreased along with time prolongation and almost terminated after 40 mins. These results indicate that active species are immediately formed when cocatalyst is added, the catalytic activity will be slowly decreased along with prolonged reaction time and the deactivation of partial active sites due to the cumulation of impurities. Therefore, further investigations of other nickel complexes are carried out with the optimum condition at Al/Ni ratio 700 at 30 °C within 30 mins.

All nickel complexes displayed high activities and good selectivity of α-olefin with a dimer as predominated product, as summarized in Table 2. To compare the environmental influence of the ligands on their catalytic activities, the title complexes were classified into two

Table 2
Ethylene catalytic activity with nickel complexes using Et$_2$AlCl[a].

Entry	Precatalyst	Al/Ni	T (°C)	t (min)	Activity[c]	Oligomer distribution[b]		
						C4/ΣC	C6/ΣC	α-Olefin (%)
1	**C4**	400	30	30	5.4	96.5	3.5	91.8
2	**C4**	600	30	30	6.6	99.1	0.9	94.3
3	**Ci4**	700	30	30	38	99.7	0.3	> 99
4	**C4**	800	30	30	6.6	96.0	4.0	96.0
5	**C4**	700	20	30	26	90.2	9.8	92.1
6	**C4**	700	40	30	23	91.6	8.4	50.7
7	**C4**	700	50	30	11	95.0	5.0	83.1
8	**C4**	700	30	10	52	99.8	0.2	> 99
9	**C4**	700	30	20	42	99.7	0.3	> 99
10	**C4**	700	30	40	30	99.7	0.3	> 99
11	**C4**	700	30	50	25	99.7	0.3	> 99
12	**C4**	700	30	60	21	99.7	0.3	> 99
13	**C1**	700	30	30	28	> 99.9	–	91.3
14	**C2**	700	30	30	25	99.4	0.6	98.1
15	**C3**	700	30	30	17	94.0	6.0	77.1
16	**C5**	700	30	30	35	94.7	5.3	21.0
17	**C6**	700	30	30	8.1	96.3	3.7	93.3
18	**C7**	700	30	30	35	99.3	0.7	60.1
19	**C8**	700	30	30	14	98.9	1.1	34.6
20	**C9**	700	30	30	8.3	97.4	2.6	12.7
21	**C10**	700	20	30	31	97.9	2.1	> 99
22	**C10**	700	30	30	52	98.8	1.2	97.0
23	**C10**	700	40	30	43	98.5	1.5	62.5
24	**C10**	700	50	30	8.4	98.9	1.1	27.4
25	**C11**	700	30	30	36	99.7	0.3	> 99
26	**C12**	700	30	30	5.6	96.6	3.4	71.0

[a] Reaction condition: 5 μmol Ni; 30 min, Et$_2$AlCl; 10 atm ethylene; 100 mL toluene.
[b] Determined by GC.
[c] 10^5 g mol^{-1}(Ni) h^{-1}.

groups based upon the anionic halides, dichlorides **C1**–**C6** and dibromides **C7**–**C12**. The complexes **C4** and **C10** bearing 2,4,6-trimethyl-substituted showed the highest catalytic activity in each group (Entries 3 and 22 respectively, Table 2). Variation of the R^1 groups at the ortho-positions of the imino-N aryl rings affects their catalytic performances, the increasing steric hindrance leads to decrease the catalytic activities in order of **C1** > **C2** > **C3** (Entries 13–15, Table 2) and **C7** > **C8** > **C9** (Entries 18–20, Table 2). With the same steric influence, the activity of complex **C4** (Entry 3, Table 2) is higher than that of complex **C5** (Entry 16, Table 2), and so is the activity of **C10** (Entry 22, Table 2) better than that of **C11** (Entry 25, Table 2). Meanwhile, complexes **C6** (Entry 17, Table 2) and **C12** (Entry 26, Table 2) containing ligands with chloro-substituents show lower catalytic activities. These phenomenon are caused by the solubility factors of nickel complexes, complexes with ligands containing additional methyl-substituents enhance their solubility, but complexes with ligands containing halides have lower solubility. The similar phenomena were also observed within complexes ligated by their analogues of the ligands [33,34].

Regarding the effects of anionic halides (chloride for **C1**–**C6** and bromides for **C7**–**C12**), the synergic influences of halides and the ligands were observed for their catalytic activities. It is common for bromide precursors showing better activity than the corresponding chlorides [26,27,38], which is attributed to better solubility of the bromo complexes. In current system, ligands containing an additional methyl group generally enhance the solubilities of all complexes, therefore, the leaving groups of anionic halides synergically affect their catalytic activities with substituents of their ligands. With ortho-methyl groups of the imino-N aryl rings (Entry 13 vs. Entry 18, and Entry 3 vs. Entry 22, Table 2), the bromonickel catalysts perform better activities than these of chloronickel complexes due to the solubility of complexes. Ethyl or iso-propyl groups at ortho-positions of the imino-N aryl rings (Entry 14 vs. Entry 19, and Entry 15 vs. Entry 20, Table 2), better activities showed for chloronickel catalyst than bromonickel catalyst, which is caused by the net charge influence on catalytic acivity [39].

As previously observed [32,33], most complexes containing N–H group on the benzimidazole showed higher activities. It is imaged that some active species of anionic amides or aluminum amides formed in situ with adding organoaluminum, based on the evidences of metallocene [40,41] and complex catalysts [13]. Due to better solubility, the title complexes performed higher activities than their analogues without methyl on the phenyl ring of the benzimidazoles [34]. This is an alternative way to modify ligands with changing its solubility for improving the catalytic activities.

3. Conclusions

A series of nickel complexes was synthesized and fully characterized. The X-ray crystallographic studies on the nickel complexes **C1** and **C3** displayed the distorted

octahedral geometry around nickel atom with incorporation of solvent molecule. All nickel complexes, activated by Et$_2$AlCl, exhibited high activities for ethylene oligomerization. Their activities were generally higher than their analogues [34] because the title complexes, containing ligands with an additional methyl group of the benzoimidazoles, have better solubility. Within present system of ligands, the bulkier substituents decrease catalytic activities. The synergic influences of ligands and anionic halides have the considerable effects on their catalytic activities.

4. Experimental

4.1. General considerations

All manipulations of air- and moisture-sensitive compounds were carried out in nitrogen atmosphere using standard Schlenk techniques. Toluene was refluxed over sodium-benzophenone and distilled under nitrogen prior to use. Diethylaluminum chloride (Et$_2$AlCl, 1.7 M in toluene) was purchased from Acros Chemicals. Other reagents were purchased from Aldrich or Acros Chemicals. ^{1}H and ^{13}C NMR spectra were recorded on a Bruker DMX 400 MHz instrument at ambient temperature using TMS as an internal standard. IR spectra were recorded on a Perkin-Elmer System 2000 FT-IR spectrometer. Elemental analysis was carried out using a Flash EA 1112 micro-analyzer. GC analysis was performed with a Varian CP-3800 gas chromatograph equipped with a flame ionization detector and a 30-m (0.2 mm i.d., 0.25 μm film thickness) CP-Sil 5 CB column. The yield of oligomers was calculated by referencing with the mass of the solvent on the basis of the prerequisite that the mass of each fraction was approximately proportional to its integrated areas in the GC trace. Selectivity for the linear α-olefin was defined as (amount of linear α-olefin of all fractions)/(total amount of oligomer products) in percent.

4.2. Preparation of the organic compounds and nickel complexes

4.2.1. Preparation of 6-(methyl-substituted-1H-benzoimidazol-2-yl)-2-acetylpyridine

According to the synthetic procedure of 6-(1H-benzoimidazol-2-yl)-2-acetylpyridine [31], a mixture of diethyl 2,6-bis(β-keto-carboxylate)pyridine [37] (9.27 g, 0.030 mol), 1.5 equivalent molar 3-methylbenzene-1,2-diamine (5.49 g, 0.045 mol), and a catalytic amount of p-toluenesulfonic acid in the 80 mL solution of toluene and isopropyl alcohol (3:1, v/v) was refluxed for 14 h. A mixture of 20 mL of acetic acid and 5 mL of concentrated HCl was added and continued to reflux for additional 6 h. The resultant solution was cooled to room temperature, a 20% KOH solution was added to neutralize the solution to the pH value between 9 and 10. The aqueous phase was extracted with ethyl acetate (20 mL × 3), all organic extracts were combined and dried over anhydrous Na$_2$SO$_4$. After drying and purification by column chromatography (alumina column 3/1 petroleum ether/ethyl acetate), the product obtained as white solids (3.77 g, 50.7% isolated yield) with the roughly molar ratio of 3:2 for 6-(7-methyl-

1H-benzoimidazol-2-yl)-2-acetylpyridine and 6-(4-methyl-1H-benzoimidazol-2-yl)-2-acetylpyridine. For combined isomers solids: Mp: 165–166 C. IR (KBr; cm^{-1}): 3414.4 (s), 3055.7 (w), 1694.3 (s), 1591 (s), 1567 (w), 1505.6 (w), 1459.6 (m), 828.2 (s), 747.1 (s). Anal. Calcd for C$_{15}$H$_{13}$N$_3$O: C, 71.70; H, 5.21; N, 16.72. Found: C, 71.42; H, 5.49; N, 16.73. 6-(7-methyl-1H-benzoimidazol-2-yl)-2-acetylpyridine: ^{1}H NMR (400 MHz, CDCl$_3$, TMS): δ 10.31 (s, 1H, NH), 8.65 (d, J = 3.9 Hz, 1H, Py), 8.03–8.11 (m, 1H, Py), 7.98–8.02 (m, 1H, Py), 7.40 (d, J = 8.1 Hz, 1H, Ph), 7.15–7.24 (m, 1H, Ph), 7.13 (t, J = 8.6 Hz, 1H, Ph), 2.86 (s, 3H, CH$_3$), 2.75 (s, 3H, CH$_3$). ^{13}C NMR (100 MHz, CDCl$_3$, TMS): δ 199.3, 153.1, 149.6, 148.1, 144.1, 138.2, 133.7, 125.0, 123.3, 122.3, 117.9, 108.9, 25.9, 17.0. 6-(4-methyl-1H-benzoimidazol-2-yl)-2-acetylpyridine: ^{1}H NMR (400 MHz, CDCl$_3$, TMS): δ 10.19 (s, 1H, NH), 8.61 (d, J = 3.9 Hz, 1H, Py), 8.03–8.11 (m, 1H, Py), 7.98–8.02 (m, 1H, Py), 7.70 (d, J = 8.1 Hz, 1H, Ph), 7.15–7.26 (m, 1H, Ph), 7.13 (t, J = 8.6 Hz, 1H, Ph), 2.86 (s, 3H, CH$_3$), 2.64 (s, 3H, CH$_3$). ^{13}C NMR (100 MHz, CDCl$_3$, TMS): δ 199.3, 153.1, 149.3, 148.1, 144.1, 138.2, 130.6, 125.0, 124.3, 122.5, 121.3, 108.9, 25.9, 17.2.

4.2.2. Synthesis of 2-(methyl-substituted-1H-benzoimidazol-2-yl)-6-(1-aryliminoethyl)pyridines (L1–L6)

6-[1-(2,6-dimethylphenylimio)ethyl]-2-(7-methyl-1H-benzoimidazol-2-yl)pyridine and 6-[1-(2,6-dimethylphenylimio)ethyl]-2-(4-methyl-1H-benzoimidazol-2-yl)pyridine (L1). A solution of precursor compounds (0.75 g, 3.0 mmol), 2,6-dimethylaniline (0.54 g, 4.50 mmol), and a catalytic amount of p-toluenesulfonic acid dissolved in toluene (25 mL) was refluxed for 24 h. After solvent evaporation, the crude product was purified by column chromatography on basic Al$_2$O$_3$ with petroleum ether/ethyl acetate (v/v, 8:1) as eluent to afford the product as a light yellow powder in 62.3% yield, with the roughly molar ratio of 3:2 for 6-[1-(2,6-dimethylphenylimio)ethyl]-2-(7-methyl-1H-benzo imidazol-2-yl)pyridine and 6-[1-(2,6-dimethylphenylimio)ethyl]-2-(4-methyl-1H-benzoimidazol-2-yl)pyridine. For combined isomers solids: Mp: 217–219 C. IR (KBr; cm^{-1}): 3641.4 (w), 3079.0 (w), 1658.3 (vs), 1595.1 (w), 1570.6 (m), 1464.1 (w), 1428.1 (m), 1313.1 (s), 822.7 (m), 755.4 (s). Anal. Calcd for C$_{23}$H$_{22}$N$_4$: C, 77.94; H, 6.26; N, 15.81. Found: C, 77.58; H, 6.49; N, 15.61. 6-[1-(2,6-dimethylphenylimio)ethyl]-2-(7-methyl-1H-benzoimidazol-2-yl)pyridine: ^{1}H NMR (400 MHz, CDCl$_3$, TMS): δ 10.45 (s, 1H, NH), 8.57 (d, J = 5.2 Hz, 1H, Py), 8.43 (d, J = 8.0 Hz, 1H, Py), 7.97–7.99 (m, 1H, Py), 7.71 (d, J = 8.0 Hz, 1H, Py), 7.19–7.23 (m, 1H, Ph), 7.08–7.11 (m, 3H, Ph), 6.93–6.96 (m, 1H, Ph), 2.62 (s, 3H, CH$_3$), 2.30 (s, 3H, CH$_3$), 2.06 (s, 6H, CH$_3$). ^{13}C NMR (100 MHz, CDCl$_3$, TMS): δ 166.5, 154.3, 150.7, 148.1, 138.4, 128.3, 128.2, 125.8, 123.9, 123.2, 109.0, 50.3, 18.1, 17.9, 15.2. 6-[1-(2,6-dimethylphenylimio)ethyl]-2-(4-methyl-1H-benzoimidazol-2-yl)pyridine: ^{1}H NMR (400 MHz, CDCl$_3$, TMS): δ 10.25 (s, 1H, NH), 8.53 (d, J = 5.5 Hz, 1H, Py), 8.43 (d, J = 8.0 Hz, 1H, Py), 7.97–7.99 (m, 1H, Py), 7.39 (d, J = 12 Hz, 1H, Ph), 7.19–7.23 (m, 1H, Ph), 7.08–7.11 (m, 3H, Ph), 6.93–6.96 (m, 1H, Ph), 2.76 (s, 3H, CH$_3$), 2.30 (s, 3H, CH$_3$), 2.06 (s, 6H, CH$_3$). ^{13}C NMR (100 MHz, CDCl$_3$, TMS): δ 166.5, 150.7, 148.8, 148.1, 138.4, 138.1, 134.5, 128.3, 128.2, 125.8, 123.9, 123.2, 117.0, 50.1, 18.1, 17.6, 15.2.

6-[1-(2,6-diethylphenylimio)ethyl]-2-(7-methyl-1H-benzoimidazol-2-yl)pyridine and 6-[1-(2,6-diethylphenylimio)ethyl]-2-(4-methyl-1H-benzoimidazol-2-yl)pyridine (L2). Using the same procedure as for L1, L2 was obtained as a light yellow powder in 78.8% yield, with the roughly molar ratio of 3:2 for 6-[1-(2,6-diethylphenylimio)ethyl]-2-(7-methyl-1H-benzoimidazol-2-yl)pyridine and 6-[1-(2,6-diethylphenylimio)ethyl]-2-(4-methyl-1H-benzoimidazol-2-yl)pyridine. For combined isomers solids: Mp: 188–189 °C. IR (KBr; cm^{-1}): 3641.4 (w), 3079.0 (w), 1658.3 (vs), 1595.1 (w), 1570.6 (m), 1464.1 (w), 1428.1 (m), 1313.1 (s), 822.7 (m), 755.4 (s). Anal. Calcd for $C_{25}H_{26}N_4$: C, 78.50; H, 6.85; N, 14.65. Found: C, 78.23; H, 7.04; N, 14.62. 6-[1-(2,6-Diethylphenylimio)ethyl]-2-(7-methyl-1H-benzoimidazol-2-yl)pyridine: ^{1}H NMR (400 MHz, CDCl$_3$, TMS): δ 10. 36 (s, 1H, NH), 8.57 (d, J = 3.9 Hz, 1H, Py), 8.43 (d, J = 7.8 Hz, 1H, Py), 7.95–8.01 (m, 1H, Py), 7.71 (d, J = 8.1 Hz, 1H, Ph), 7.20–7.24 (m, 1H, Ph), 7.13–7.15 (m, 3H, Ph), 7.04–7.08 (m, 1H, Ph), 2.77 (s, 3H, CH$_3$), 2.35–2.48 (m, 4H, CH$_2$), 2.32 (s, 3H, CH$_3$), 1.16 (t, J = 7.5 Hz, 6H, CH$_3$). ^{13}C NMR (100 MHz, CDCl$_3$, TMS): δ 166.2, 156.0, 147.7, 144.3, 137.9, 133.6, 133.3, 130.5, 126.1, 124.0, 123.1, 122.8, 122.3, 122.1, 117.8, 108.8, 24.4, 17.1, 13.9, 13.2. 6-[1-(2,6-diethylphenylimio)ethyl]-2-(4-methyl-1H-benzoimidazol-2-yl)pyridine: ^{1}H NMR (400 MHz, CDCl$_3$, TMS): δ 10.27 (s, 1H, NH), 8.53 (d, J = 3.9 Hz, 1H, Py), 8.43 (d, J = 7.8 Hz, 1H, Py), 7.95–8.01 (m, 1H, Py), 7.38 (d, J = 8.1 Hz, 1H, Ph), 7.20–7.24 (m, 1H, Ph), 7.13–7.15 (m, 3H, Ph), 7.04–7.08 (m, 1H, Ph), 2.63 (s, 3H, CH$_3$), 2.35–2.48 (m, 4H, CH$_2$), 2.32 (s, 3H, CH$_3$), 1.16 (t, J = 7.5 Hz, 6H, CH$_3$). ^{13}C NMR (100 MHz, CDCl$_3$, TMS): δ 166.2, 156.0, 150.0, 147.6, 144.2, 137.8, 133.6, 131.3, 130.5, 126.1, 124.0, 123.6, 123.1, 122.3, 122.2, 117.8, 108.8, 24.4, 17.1, 13.9, 13.2.

6-[1-(2,6-diisopropylphenylimio)ethyl]-2-(7-methyl-1H-benzoimidazol-2-yl)pyridine and 6-[1-(2,6-diisopropylphenylimio)ethyl]-2-(4-methyl-1H-benzoimidazol-2-yl)pyridine (L3). Using the same procedureas for the L1, L3 was obtained as a light yellow powder in 81.3% yield, with the roughly molar ratio of 3:2 for 6-[1-(2,6-diisopropylphenylimio)ethyl]-2-(7-methyl-1H-benzoimidazol-2-yl)pyridine and 6-[1-(2,6-diisopropylphenylimio)ethyl]-2-(4-methyl-1H-benzoimidazol-2-yl)pyridine. For combined isomers solids: Mp: 201–202 °C. IR (KBr; cm^{-1}): 3457.8 (m), 3058.1 (w), 2962.9 (m), 1645.0 (vs), 1591.4 (s), 1567.8 (s), 1461.3 (m), 1431.1 (m), 1316.1 (s), 905.7 (s), 755.8 (s). Anal. Calcd for $C_{27}H_{30}N_4$: C, 78.99; H, 7.37; N, 13.65. Found: C, 78.61; H, 7.37; N, 13.36. 6-[1-(2,6-diisopropylphenylimio)ethyl]-2-(7-methyl-1H-benzoimidazol-2-yl)pyridine: ^{1}H NMR (400 MHz, CDCl$_3$, TMS): δ 10.45 (s, 1H, NH), 8.57 (d, J = 3.9 Hz, 1H, Py), 8.41–8.45 (m, 1H, Py), 7.98 (d, J = 3.7 Hz, 1H, Py), 7.25 (d, J = 4.5 Hz, 1H, Ph), 7.18–7.20 (m, 3H, Ph), 7.10–7.15 (m, 2H, Ph), 2.74–2.80 (m, 2H, CH), 2.62 (s, 3H, CH$_3$), 2.33 (s, 3H, CH$_3$), 1.17 (d, J = 3.9 Hz, 12H, CH$_3$). ^{13}C NMR (100 MHz, CDCl$_3$, TMS): δ 166.4, 155.9, 150.3, 147.7, 144.3, 138.0, 133.6, 131.3, 126.1, 124.7, 123.6, 123.1, 122.8, 122.3, 122.2, 117.8, 108.8, 24.7, 17.1, 17.0, 13.8. 6-[1-(2,6-Diisopropylphenylimio)ethyl]-2-(4-methyl-1H-benzoimidazol-2-yl)pyridine: ^{1}H NMR (400 MHz, CDCl$_3$, TMS): δ 10.32 (s, 1H, NH), 8.54 (d, J = 3.9 Hz, 1H, Py), 8.41–8.45 (m, 1H, Py), 7.98 (d, J = 3.7 Hz, 1H, Py), 7.38 (d, J = 4.0 Hz, 1H, Ph), 7.18–7.20 (m, 3H, Ph), 7.10–7.15 (m, 2H, Ph), 2.77 (s, 3H, CH$_3$), 2.74–2.80 (m, 2H, CH), 2.33 (s, 3H, CH$_3$), 1.17 (d, J = 3.9 Hz, 12H, CH$_3$). ^{13}C NMR (100 MHz, CDCl$_3$, TMS): δ 166.4, 155.9, 150.1, 147.6, 144.2, 137.8, 133.6, 131.3, 126.1, 124.0, 123.6, 123.1, 122.8, 122.1, 121.3, 117.8, 108.8, 24.7, 17.2, 17.0, 13.0.

6-[1-(2,4,6-trimethylphenylimio)ethyl]-2-(7-methyl-1H-benzoimidazol-2-yl)pyridine and 6-[1-(2,4,6-trimethylphenylimio)ethyl]-2-(4-methyl-1H-benzoimidazol-2-yl)pyridine (L4). Using the same procedure as for L1, L4 was obtained as a light yellow powder in 68.7% yield, with the roughly molar ratio of 3:2 for 6-[1-(2,4,6-trimethylphenylimio)ethyl]-2-(7-methyl-1H-benzoimidazol-2-yl)pyridine and 6-[1-(2,4,6-trimethylphenylimio)ethyl]-2-(4-methyl-1H-benzoimidazol-2-yl)pyridine. For combined isomers solids: Mp: 170 °C. IR (KBr; cm^{-1}): 3459.6 (w), 2918.5 (m), 1646.8 (vs), 1592.0 (m), 1568.5 (s), 1465.3 (m), 1428.5 (m), 1323.8 (s), 1125.0 (m), 853.6 (s), 823.5 (m), 753.2 (s). Anal. Calcd for $C_{24}H_{24}N_4$: C, 78.23; H, 6.57; N, 15.21. Found: C, 78.22; H, 6.94; N, 14.95. 6-[1-(2,4,6-trimethylphenylimio)ethyl]-2-(7-methyl-1H-benzoimidazol-2-yl)pyridine: ^{1}H NMR (400 MHz, CDCl$_3$, TMS): δ 10.43 (s, 1H, NH), 8.56 (d, J = 3.9 Hz, 1H, Py), 8.40 (t, J = 8.1 Hz, 1H, Py), 7.96–7.98 (m, 1H, Py), 7.71 (d, J = 8.3 Hz, 1H, Ph), 7.20–7.23 (m, 1H, Ph), 7.12 (t, J = 5.9 Hz, 1H, Ph), 6.92 (s, 2H, Ph), 2.62 (s, 3H, CH$_3$), 2.31 (s, 3H, CH$_3$), 2.30 (s, 3H, CH$_3$), 2.03 (s, 6H, CH$_3$). ^{13}C NMR (100 MHz, CDCl$_3$, TMS): δ 166.7, 156.1, 150.5, 147.6, 146.1, 144.1, 137.8, 133.8, 132.6, 130.4, 128.8, 125.3, 124.0, 123.1, 122.8, 121.3, 117.7, 108.9, 22.8, 20.9, 18.0, 17.7, 16.8. 6-[1-(2,4,6-trimethylphenylimio)ethyl]-2-(4-methyl-1H-benzoimidazol-2-yl)pyridine: ^{1}H NMR (400 MHz, CDCl$_3$, TMS): δ 10.38 (s, 1H, NH), 8.52 (d, J = 4.0 Hz, 1H, Py), 8.40 (t, J = 8.1 Hz, 1H, Py), 7.96–7.98 (m, 1H, Py), 7.39 (d, J = 8.3 Hz, 1H, Ph), 7.20–7.23 (m, 1H, Ph), 7.12 (t, J = 5.9 Hz, 1H, Ph), 6.92 (s, 2H, Ph), 2.76 (s, 3H, CH$_3$), 2.31 (s, 3H, CH$_3$), 2.30 (s, 3H, CH$_3$), 2.03 (s, 6H, CH$_3$). ^{13}C NMR (100 MHz, CDCl$_3$, TMS): δ 166.7, 156.1, 150.2, 147.6, 146.2, 144.1, 137.7, 133.8, 132.6, 130.4, 128.8, 125.3, 124.0, 123.1, 122.8, 121.3, 117.7, 108.9, 22.8, 20.9, 18.0, 17.1, 16.7.

6-[1-(2,6-diethyl-4-methylphenylimio)ethyl]-2-(7-methyl-1H-benzoimidazol-2-yl)pyridine and 6-[1-(2,6-diethyl-4-methylphenylimio)ethyl]-2-(4-methyl-1H-benzoimidazol-2-yl)pyridine (L5). Using the same procedure as for L1, L5 was obtained as a light yellow powder in 65.3% yield, with the roughly molar ratio of 3:2 for 6-[1-(2,6-diethyl-4-methylphenylimio)ethyl]-2-(7-methyl-1H-benzo imidazol-2-yl)pyridine and 6-[1-(2,6-diethyl-4-methylphenylimio)ethyl]-2-(4-methyl-1H-benzoimidazol-2-yl)pyridine. For combined isomers solids: Mp: 200–202 °C. IR (KBr; cm^{-1}): 3458.0 (m), 2981.4 (m), 1645.2 (vs), 1568.2 (s), 1473.2 (m), 1443.8 (m), 1316.6 (s), 1210.2 (s), 990.0 (m), 858.8 (m), 752.0 (s). Anal. Calcd for $C_{26}H_{28}N_4$: C, 78.75; H, 7.12; N, 14.13. Found: C, 78.85; H, 7.18; N, 13.97. 6-[1-(2,6-diethyl-4-methylphenylimio)ethyl]-2-(7-methyl-1H-benzoimidazol-2-yl)pyridine: ^{1}H NMR (400 MHz, CDCl$_3$, TMS): δ 10.35 (s, 1H, NH), 8.56 (d, J = 3.9 Hz, 1H, Py), 8.41 (d, J = 7.7 Hz, 1H, Py), 7.96–7.98 (m, 1H, Py), 7.71 (d, J = 8.1 Hz, 1H, Ph), 7.20–7.24 (m, 1H, Ph), 7.12 (t, J = 6.4 Hz, 1H, Ph), 6.95 (s, 2H, Ph), 2.62 (s, 3H, CH$_3$), 2.39–2.43 (m, 4H, CH$_2$), 2.35 (s, 3H, CH$_3$), 2.32 (s, 3H, CH$_3$), 1.15 (t, J = 7.5 Hz, 6H, CH$_3$). ^{13}C NMR (100 MHz, CDCl$_3$, TMS): δ 166.5, 156.1,

150.4, 147.5, 145.1, 144.1, 137.7, 133.6, 132.7, 131.0, 130.3, 126.8, 124.6, 122.9, 122.6, 122.2, 117.7, 108.8, 24.6, 21.0, 17.1, 17.0, 13.9. 6-[1-(2,6-diethyl-4-methylphenyli-mio)ethyl]-2-(4-methyl-1H-benzoimidazol-2-yl)pyridine: ^{1}H NMR (400 MHz, CDCl$_3$, TMS): δ 10.21 (s, 1H, NH), 8.52 (d, J = 3.9 Hz, 1H, Py), 8.41 (d, J = 7.7 Hz, 1H, Py), 7.96–7.98 (m, 1H, Py), 7.38 (d, J = 7.9 Hz, 1H, Ph), 7.20–7.24 (m, 1H, Ph), 7.12 (t, J = 6.4 Hz, 1H, Ph), 6.95 (s, 2H, Ph), 2.77 (s, 3H, CH$_3$), 2.39–2.43 (m, 4H, CH$_2$), 2.35 (s, 3H, CH$_3$), 2.32 (s, 3H, CH$_3$), 1.15 (t, J = 7.5 Hz, 6H, CH$_3$). ^{13}C NMR (100 MHz, CDCl$_3$, TMS): δ 166.5, 156.1, 150.1, 147.5, 145.1, 144.0, 137.6, 133.6, 132.6, 131.0, 130.3, 126.7.

6-[1-(2,6-dichlorophenylimio)ethyl]-2-(7-methyl-1H-benzoimidazol-2-yl)pyridine and 6-[1-(2,6-dichlorophe-nylimio)ethyl]-2-(4-methyl-1H-benzoimidazol-2-yl)pyri-dine (**L6**). Using a similar procedure as for **L1**, but using silicic acid tetraethyl ester as a solvent instead of toluene, **L6** was obtained as a white powder in 38.3% yield, with the ougly molar ratio of 3:2 for 6-[1-(2,6-dichlorophenyli-mio)ethyl]-2-(7-methyl-1H-benzoimidazol-2-yl)pyridine and 6-[1-(2,6-dichlorophenylimio)ethyl]-2-(4-methyl-1H-benzoimidazol-2-yl)pyridine. For combined isomers solids: Mp: 235 °C. IR (KBr; cm^{-1}): 3464.3 (m), 3082.9 (w), 1663.0 (vs), 1593.1 (m), 1568.9 (m), 1461.8 (m), 1224.3 (m), 822.0 (m). Anal. Calcd for C$_{21}$H$_{16}$N$_4$Cl$_2$: C, 63.81; H, 4.08; N, 14.17. Found: C, 63.84; H, 4.10; N, 13.83. 6-[1-(2,6-dichlorophenylimio)ethyl]-2-(7-methyl-1H-benzo imidazol-2-yl)pyridine: ^{1}H NMR (400 MHz, CDCl$_3$, TMS): δ 10.36 (s, 1H, NH), 8.59 (d, 1H, J = 3.9 Hz, Py), 8.43 (d, 1H, J = 7.8 Hz, Py), 7.99–8.02 (m, 1H, Py), 7.71 (d, 1H, J = 8.1 Hz, Ph), 7.39 (d, 3H, J = 8.0 Hz, Ph), 7.18–7.24 (m, 1H, Ph), 7.10–7.14 (t, 1H, J = 6.7 Hz, Ph), 7.00–7.04 (m, 1H, Ph), 2.62 (s, 3H, CH$_3$), 2.42 (s, 3H, CH$_3$). ^{13}C NMR (100 MHz, CDCl$_3$, TMS): δ 170.8, 155.2, 150.0, 147.7, 145.5, 144.1, 137.9, 130.5, 128.3, 124.6, 124.1, 123.1, 122.7, 108.8, 17.9, 17.0. 6-[1-(2,6-dichlorophenylimio)ethyl]-2-(4-methyl-1H-benzoimidazol-2-yl)pyridine: ^{1}H NMR (400 MHz, CDCl$_3$, TMS): δ 10.26 (s, 1H, NH), 8.56 (d, 1H, J = 3.9 Hz, Py), 8.43 (d, 1H, J = 7.8 Hz, Py), 7.99–8.02 (m, 1H, Py), 7.39 (d, 2H, J = 8.0 Hz, Ph), 7.18–7.24 (m, 1H, Ph), 7.10–7.14 (t, 1H, J = 6.7 Hz, Ph), 7.00–7.04 (m, 1H, Ph), 2.76 (s, 3H, CH$_3$), 2.42 (s, 3H, CH$_3$). ^{13}C NMR (100 MHz, CDCl$_3$, TMS): δ 170.8, 155.2, 159.9, 147.7, 145.5, 144.1, 137.9, 133.7, 128.3, 124.6, 123.5, 122.8, 108.8, 17.9, 17.0.

4.2.3. Synthesis of tridentate nickel complexes C1–C12

Nickel complexes **C1**–**C12** were prepared by the same synthetic procedures and obtained as a yellow powder. The synthetic procedure for **C1** can be described as follows: to a mixture of ligand **L1** (0.124 g, 0.35 mmol) and NiCl$_2$. 4H$_2$O (0.083 g, 0.35 mmol) was added freshly prepared distilled ethanol (5 mL) at room temperature. The solution turned yellow immediately. The reaction mixture was stirred for 10 h, and the precipitate was collected by filtration and washed with diethyl ether, followed by drying in vacuum. The target complex was obtained as a yellow powder in 87.6% yield. IR (KBr; cm^{-1}): 3496.3 (w), 2975.3 (w), 1599.6 (vs), 1476.7 (m), 1424.1 (m), 1317.6 (m), 817.0 (s), 750.4 (s). Anal. Calcd for C$_{23}$H$_{22}$Cl$_2$N$_4$Ni: C, 57.07; H, 4.58; N, 11.57. Found: C, 56.77; H, 4.72; N, 11.90.

Data for **C2** Yield: 84.1%. IR (KBr; cm^{-1}): 3420.1 (w), 3046.6 (w), 2971.7 (w), 1598.8 (vs), 1449.1 (m), 1377.6 (s), 1317.7 (s), 1158.1 (m), 794.6 (s), 752.4 (s). Anal. Calcd for C$_{25}$H$_{26}$Cl$_2$NiN$_4$: C, 58.63; H, 5.12; N, 10.94. Found: C, 58.77; H, 5.17; N, 10.72.

Data for **C3** Yield: 90.1%. IR (KBr; cm^{-1}): 3390.0 (m), 3058.4 (m), 2966.0 (m), 1591.0 (vs), 1472.0 (w), 1444.9 (w), 1319.5 (s), 1202.7 (s), 816.9 (m), 766.7 (s), 746.1 (s). Anal. Calcd for C$_{27}$H$_{30}$Cl$_2$NiN$_4$: C, 60.04; H, 5.60; N, 10.37. Found: C, 60.11; H, 5.61; N, 10.22.

Data for **C4** Yield: 88.7%. IR (KBr; cm^{-1}): 3467.8 (w), 3017.4 (w), 1597.9 (vs), 1445.9 (m), 1319.1 (s), 1197.2 (s), 823.4 (m), 792.4 (s), 760.7 (m). Anal. Calcd for C$_{24}$H$_{24}$Cl$_2$NiN$_4$: C, 57.87; H, 4.86; N, 11.25. Found: C, 57.53; H, 5.10; N, 11.06.

Data for **C5** Yield: 85.3%. IR (KBr; cm^{-1}): 3282.5 (m), 3114.0 (m), 2968.5 (m), 1598.6 (vs), 1479.4 (m), 1457.0 (m), 1422.5 (m), 1316.6 (s), 1087.4 (m), 1042.4 (s), 814.6 (s), 750.5 (s). Anal. Calcd for C$_{26}$H$_{28}$Cl$_2$NiN$_4$: C, 59.35; H, 5.36; N, 10.65. Found: C, 59.00; H, 5.28; N, 10.35.

Data for **C6** Yield: 67.5%. IR (KBr; cm^{-1}): 3362.3 (m), 3084.3 (w), 1599.9 (vs), 1478.2 (w), 1409.8 (vs), 1316.6 (s), 1277.5 (s), 819.2 (m), 789.8 (s). Anal. Calcd for C$_{21}$H$_{16}$Cl$_4$NiN$_4$: C, 48.05; H, 3.07; N, 10.67. Found: C, 47.86; H, 3.43; N, 10.46.

Data for **C7** Yield: 94.9%. IR (KBr; cm^{-1}): 3268.9 (s), 1599.8 (vs), 1475.9 (m), 1420.9 (m), 1316.6 (s), 1209.6 (s), 816.4 (m), 788.5 (w). Anal. Calcd for C$_{23}$H$_{22}$Br$_2$NiN$_4$: C, 48.21; H, 3.87; N, 9.78. Found: C, 48.51; H, 3.99; N, 9.53.

Data for **C8** Yield: 91.7%. IR (KBr; cm^{-1}): 3278.9 (s), 1599.5 (vs), 1475.0 (m), 1419.2 (m), 1316.4 (s), 1271.5 (s), 868.4 (w), 793.4 (m), 747.8 (m). Anal. Calcd for C$_{25}$H$_{26}$Br$_2$NiN$_4$: C, 49.96; H, 4.36; N, 9.32. Found: C, 49.65; H, 4.17; N, 9.68.

Data for **C9** Yield: 89.4%. IR (KBr; cm^{-1}): 3381.5(m), 3054.9(w), 1597.0(vs), 1461.3(m), 1422.6(m), 1316.8(s), 1205.4(m), 816.6(m), 766.3(s). Anal. Calcd for C$_{27}$H$_{30}$Br$_2$NiN$_4$: C, 51.55; H, 4.81; N, 8.91. Found: C, 51.81; H, 5.01; N, 8.65.

Data for **C10** Yield: 93.7%. IR (KBr; cm^{-1}): 3245.7 (s), 1600.7 (vs), 1477.7 (s), 1419.8 (w), 1316.5 (s), 1238.0 (m), 1216.5 (s), 856.0 (m), 788.4 (s), 749.0 (m). Anal. Calcd for C$_{24}$H$_{24}$Br$_2$NiN$_4$: C, 49.11; H, 4.12; N, 9.54. Found: C, 49.37; H, 4.38; N, 9.25.

Data for **C11** Yield: 86.8%. IR (KBr; cm^{-1}): 3308.7 (s), 1600.4 (vs), 1476.6 (w), 1417.4 (m), 1315.5 (s), 1273.4 (m), 1212.5 (m), 814.5 (m), 788.9 (s), 749.7 (s). Anal. Calcd for C$_{26}$H$_{28}$Br$_2$NiN$_4$: C, 50.77; H, 4.59; N, 9.11. Found: C, 50.38; H, 4.63; N, 9.41.

Data for **C12** Yield: 72.4%. IR (KBr; cm^{-1}): 3278.3 (s), 3067.2 (w), 1599.8 (vs), 1466.0 (m), 1413.2 (s), 1315.1 (s), 1210.2 (m), 933.0 (s), 806.2 (s), 740.3 (m). Anal. Calcd for C$_{21}$H$_{16}$Br$_2$Cl$_2$NiN$_4$: C, 41.09; H, 2.63; N, 9.13. Found: C, 41.28; H, 2.67; N, 8.85.

4.3. Procedure for ethylene oligomerization

Ethylene oligomerization was performed in a stainless steel autoclave (0.5 L capacity) equipped with a gas ballast through a solenoid clave for continuous feeding of ethylene at constant pressure. A 100 mL amount of toluene

Table 3
Crystal data and structure refinement for [**C1·CH₃OH**]·**CH₃OH**, **C3·CH₃OH** and [**L3NiBr₂CH₃OH**]**Br**.

	[C1·CH₃OH]·CH₃OH	C3·CH₃OH	[L3NiBr₂CH₃OH]Br
Empirical formula	$C_{25}H_{30}Cl_2N_4NiO_2$	$C_{28}H_{34}Cl_2N_4NiO$	$C_{29}H_{38}Br_2N_4NiO_2$
Formula weight	548.14	572.0	693.16
Temperature [K]	173(2) K	173 (2) K	173 (2) K
Wavelength [Å]	0.71073	0.71073	0.71073
Crystal system	Monoclinic	Monoclinic	Triclinic
Space group	P2(1)/n	P2(1)/c	P-1
a [Å]	6.8170(14)	14.330(3)	9.3652(19)
b [Å]	20.386(4)	11.022(2)	10.904(2)
c [Å]	18.047(4)	18.306(4)	17.576(4)
α [°]	90	90	91.64(3)
β [°]	93.30	112.33(3)	94.54(3)
γ [°]	90	90	97.71(3)
V [Å³]	2503.8(9)	2674.5(9)	1771.7(6)
Z, Dcalcd. [gcm⁻³]	4, 1.454	4, 1.421	2, 1.299
μ [mm⁻¹]	1.019	0.954	2.830
F(000)	1144	1200	708
Crystal size [mm]	$0.19 \times 0.07 \times 0.04$	$0.20 \times 0.20 \times 0.20$	$0.20 \times 0.20 \times 0.20$
θ range [°]	1.51–25.50	1.54–27.48	1.16–27.49
Limiting indices	$-8 \leq h \leq 8$	$-18 \leq h \leq 18$	$-11 \leq h \leq 12$
	$-24 \leq k \leq 24$	$-14 \leq k \leq 14$	$-14 \leq k \leq 14$
	$0 \leq l \leq 21$	$-22 \leq l \leq 23$	$-22 \leq l \leq 22$
Reflections collected	17274	21196	21779
Independent reflections	4643 [R(int) = 0.0760]	6075 [R(int) = 0.0374]	8084 [R(int) = 0.0368]
No. of parameters	316	327	355
Completeness to θ [%]	99.8%	99.2%	99.4%
Goodness of fit on F^2	1.258	1.253	1.113
Final R indices [$I > 2\sigma(I)$]	R1 = 0.0796	R1 = 0.0522	R1 = 0.0562
	wR2 = 0.1923	wR2 = 0.1530	wR2 = 0.1680
R indices (all data)	R1 = 0.0905	R1 = 0.0580	R1 = 0.0664
	wR2 = 0.2005	wR2 = 0.1660	wR2 = 0.1763
Max./min. $\Delta\rho$[a] [eÅ⁻³]	0.965 and −0.557	0.494 and −0.611	1.185 and −0.863

containing the complex and the required amount of cocatalyst was transferred into the fully dried reactor via a syringe under a nitrogen atmosphere. At the reaction temperature, the reactor was sealed and pressurized to high ethylene pressure, and the ethylene pressure was maintained during feeding of ethylene. After the reaction mixture was stirred for the desired period, the pressure was released and a small amount of the reaction solution was collected, which was then analyzed by gas chromatography (GC) to determine the composition and mass distribution of the oligomers obtained. To keep the reaction temperature constant, the autoclave is equipped with inert heat exchange tube of water.

4.4. X-ray crystallographic studies

All of the crystals of [**C1·CH₃OH**]·**CH₃OH**, **C3·CH₃OH** and [**L3NiBr₂CH₃OH**]**Br** suitable for X-ray diffraction analysis were obtained by laying diethyl ether on a methanol solution at room temperature. With graphite-monochromated Mo Ka radiation (λ = 0.71073 Å) at 173(2) K, cell parameters were obtained by global refinement of the positions of all collected reflections. Intensities were corrected for Lorentz and polarization effects and empirical absorption. The structures were solved by direct methods and refined by full-matrix least squares on F^2. All hydrogen atoms were placed in calculated positions. Structure solution and refinement were performed by using the SHELXL-97 package [42]. Details of the X-ray structure determinations and refinements are provided in Table 3. Crystallographic data have been deposited with the Cambridge Crystallographic Data Centre, CCDC 749265 ([**C1CH₃OH**]·**CH₃OH**), 749266 (**C3CH₃OH**) and 755621 ([**L3NiBr₂CH₃OH**]**Br**), which could be obtained free of charge from The Director, CCDC, 12 Union Road, Cambridge CB2 1EZ, UK (e-mail: deposit@ccdc.cam.ac.uk; web: http://www.ccdc.cam.ac.uk).

References

[1] W. Keim, R. Appel, A. Storeck, C. Krüger, R. Goddard, Angew. Chem. Int. Ed. Engl. 20 (1981) 116.
[2] W. Keim, Angew. Chem. Int. Ed. Engl. 29 (1990) 235.
[3] W. Keim, F.H. Kowaldt, R. Goddard, C. Krüger, Angew. Chem. Int. Ed. Engl. 17 (1978) 466.
[4] W. Keim, A. Behr, B. Limbäcker, C. Krüger, Angew. Chem. Int. Ed. Engl. 22 (1983) 503.
[5] L.K. Johnson, C.M. Killan, M. Brookhart, J. Am. Chem. Soc. 117 (1995) 6414.
[6] S.D. Ittel, L.K. Johnson, M. Brookhart, Chem. Rev. 100 (2000) 1169.
[7] V.C. Gibson, S.K. Spitzmesser, Chem. Rev. 103 (2003) 283.
[8] Z. Weng, S. Teo, T.S.A. Hor, Organometallics 25 (2006) 4878.
[9] C.M. Killian, D.J. Tempel, L.K. Johnson, M. Brookhart, J. Am. Chem. Soc. 118 (1996) 11664.
[10] S.A. Svejda, M. Brookhart, Organometallics 18 (1999) 65.
[11] Z. Guan, W.J. Marshall, Organometallics 21 (2002) 3580.
[12] A. Kermagoret, P. Braunstein, Dalton Trans. 12 (2008) 1564.

[13] F. Speiser, P. Braunstein, L. Saussine, R. Welter, Inorg. Chem. 43 (2004) 1649.
[14] X. Tang, D. Zhang, S. Jie, W.H. Sun, J. Chen, J. Organomet. Chem. 690 (2005) 3918.
[15] W.H. Sun, S. Jie, S. Zhang, W. Zhang, Y. Song, H. Ma, J. Chen, K. Wedeking, R. Fröhlich, Organometallics 25 (2006) 666.
[16] K. Wang, K. Wedeking, W. Zuo, D. Zhang, W.H. Sun, J. Organomet. Chem. 693 (2008) 1073.
[17] L. Wang, W.H. Sun, L. Han, H. Yang, Y. Hu, X. Jin, J. Organomet. Chem. 658 (2002) 62.
[18] S. Jie, S. Zhang, W.H. Sun, Eur. J. Inorg. Chem. 35 (2007) 5584.
[19] S. Zhang, I. Vystorop, Z. Tang, W.H. Sun, Organometallics 26 (2007) 2456.
[20] W.H. Sun, P. Hao, S. Zhang, Q. Shi, W. Zuo, X. Tang, X. Lu, Organometallics 26 (2007) 2720.
[21] F.A. Kunrath, R.F. De Souza, O.L. Casagrande Jr., N.R. Brooks, V.G. Young Jr., Organometallics 22 (2003) 4739.
[22] N. Ajellal, M.C.A. Kuhn, A.D.G. Boff, M. Hörner, C.M. Thomas, J.F. Carpentier, O.L. Casagrande Jr., Organometallics 25 (2006) 1213.
[23] S. Al-Benna, M.J. Sarsfield, M. Thornton-Pett, D.L. Ormsby, P.J. Maddox, P. Brés, M. Bochmann, J. Chem. Soc. Dalton Trans. 23 (2000) 4247.
[24] S.O. Ojwach, I.A. Guzei, L.L. Benade, S.F. Mapolie, J. Darkwa, Organometallics 28 (2009) 2127.
[25] A.P. Armitage, Y.D.M. Champouret, H. Grigoli, J.D.A. Pelletier, K. Singh, G.A. Solan, Eur. J. Inorg. Chem. 29 (2008) 4597.
[26] S. Adewuyi, G. Li, S. Zhang, W. Wang, P. Hao, W.H. Sun, N. Tang, J. Yi, J. Organomet. Chem. 692 (2007) 3532.
[27] M. Zhang, S. Zhang, P. Hao, S. Jie, W.H. Sun, P. Li, X. Lu, Eur. J. Inorg. Chem. 24 (2007) 3816.
[28] S. Zhang, W.H. Sun, X. Kuang, I. Vystorop, J. Yi, J. Organomet. Chem. 692 (2007) 5307.
[29] W.H. Sun, K. Wang, K. Wedeking, D. Zhang, S. Zhang, J. Cai, Y. Li, Organometallics 26 (2007) 4781.
[30] R. Gao, M. Zhang, T. Liang, F. Wang, W.H. Sun, Organometallics 27 (2008) 5641.
[31] L. Xiao, R. Gao, M. Zhang, Y. Li, X. Cao, W.H. Sun, Organometallics 28 (2009) 2225.
[32] P. Hao, S. Zhang, W.H. Sun, Q. Shi, S. Adewuyi, X. Lu, P. Li, Organometallics 26 (2007) 2439.
[33] Y. Chen, P. Hao, W. Zuo, K. Gao, W.H. Sun, J. Organomet. Chem. 693 (2008) 1829.
[34] L. Xiao, M. Zhang, R. Gao, X. Cao, W.H. Sun, Aust. J. Chem. 63 (2010) 109.
[35] L. Xiao, M. Zhang, W.H. Sun, Polyhedron 29 (2010) 142.
[36] Y. Chen, W. Zuo, P. Hao, S. Zhang, K. Gao, W.H. Sun, J. Organomet. Chem. 693 (2008) 750.
[37] M. Asma, S. Adewuyi, X. Kuang, A. Badshah, W.H. Sun, Lett. Org. Chem. 5 (2008) 296.
[38] C. Zhang, W.H. Sun, Z. Wang, Eur. J. Inorg. Chem. 23 (2006) 4895.
[39] T. Zhang, W.H. Sun, T. Li, X. Yang, J. Mol. Catal. A Chem. 218 (2004) 119.
[40] M. Bochmann, J. Organomet. Chem. 689 (2004) 3982.
[41] C. Alonso-Moreno, S.J. Lancaster, J.A. Wright, D.L. Hughes, D. Zuccaccia, A. Correa, A. Macchioni, L. Cavallo, M. Bochmann, Organometallics 27 (2008) 5474.
[42] G.M. Sheldrick, SHELXTL-97, Program for the Refinement of Crystal Structures, University of Göttingen, Germany, 1997.